

VIEWPOINT

Regulation of ion transport from within ion transit pathways

Donald W. Hilgemann 

All cells must control the activities of their ion channels and transporters to maintain physiologically appropriate gradients of solutes and ions. The complexity of underlying regulatory mechanisms is staggering, as exemplified by insulin regulation of transporter trafficking. Simpler strategies occur in single-cell organisms, where subsets of transporters act as solute sensors to regulate expression of their active homologues. This Viewpoint highlights still simpler mechanisms by which Na transporters use their own transport sites as sensors for regulation. The underlying principle is inherent to Na/K pumps in which aspartate phosphorylation and dephosphorylation are controlled by occupation of transport sites for Na and K, respectively. By this same principle, Na binding to transport sites can control intrinsic inactivation reactions that are in turn modified by extrinsic signaling factors. Cardiac Na/Ca exchangers (NCX1s) and Na/K pumps are the best examples. Inactivation of NCX1 occurs when cytoplasmic Na sites are fully occupied and is regulated by lipid signaling. Inactivation of cardiac Na/K pumps occurs when cytoplasmic Na-binding sites are not fully occupied, and inactivation is in turn regulated by Ca signaling. Potentially, Na/H exchangers (NHEs) and epithelial Na channels (ENaCs) are regulated similarly. Extracellular protons and cytoplasmic Na ions oppose secondary activation of NHEs by cytoplasmic protons. ENaCs undergo inactivation as cytoplasmic Na rises, and small diffusible molecules of an unidentified nature are likely involved. Multiple other ion channels have recently been shown to be regulated by transiting ions, thereby underscoring that ion permeation and channel gating need not be independent processes.

Introduction

Most of us learned about ion transporters in a physiology class with the help of cartoons similar to the one shown in Fig. 1. This drawing depicts the function of three powerful Na transporters in cardiac myocytes (Hilgemann et al., 2006). In brief, myocytes, like all cells in the body, use Na/K pumps to make Na and K gradients that are then used by ion channels and other transporters to carry out important functions, such as the generation of action potentials. The Na gradient is used by Na/Ca exchange (NCX) to make Ca gradients (Ottolia and Philipson, 2013) and by Na/H exchangers (NHEs) to extrude excessive protons (Lee et al., 2013). These transporters are working continuously throughout the life of a myocyte to maintain ion gradients that are appropriate for normal myocyte functions, such as excitation and contraction. They do so by an alternating access mechanism that operates with a roughly fixed stoichiometry, as indicated. That much is clear, but the transporters cannot be continuously active as suggested in this diagram.

In contradiction to the impression made in Fig. 1, ion pumps and transporters are with certainty not continuously active. Two key issues requiring more attention by the transport field for

decades are how the concentrations of the key cytoplasmic ions are sensed by cells and how that sensing is used to regulate ion transport. One solution can be that cells use specific sensors for specific ions, such as calmodulin or other proteins with Ca-binding C2 domains, and this certainly occurs prodigiously in cells. In this context, evidence that many G-proteins are regulated by binding monovalent cations (Ash et al., 2012) has received extraordinarily little attention by the transport field. A very different possibility realized in unicellular organisms is that subsets of transporters evolved to become dedicated nutrient sensors (Forsberg and Ljungdahl, 2001). By controlling expression programs, the nutrient sensors appropriately regulate the overall function of nutrient transport to meet the cell's nutrient needs.

A less appreciated regulatory possibility, highlighted in this Viewpoint, is that ion binding by the same sites used to transport ions or solutes may be used to regulate transport activity. The physical basis for such self-regulatory reactions is apparent in the normal operation of the Na/K pump (Clausen et al., 2017). Conformational changes associated with binding three Na ions control in a complex but highly reliable manner the function of

University of Texas Southwestern Medical Center, Dallas, TX.

Correspondence to Donald W. Hilgemann: donald.hilgemann@utsouthwestern.edu.

© 2019 Hilgemann. This article is distributed under the terms of an Attribution–Noncommercial–Share Alike–No Mirror Sites license for the first six months after the publication date (see <http://www.rupress.org/terms/>). After six months it is available under a Creative Commons License (Attribution–Noncommercial–Share Alike 4.0 International license, as described at <https://creativecommons.org/licenses/by-nc-sa/4.0/>).

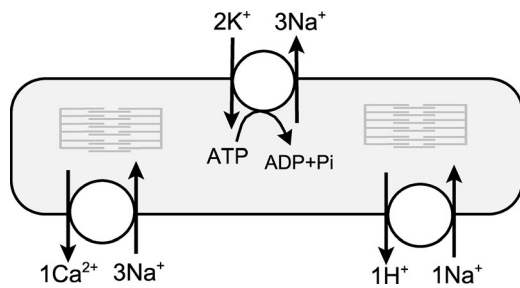


Figure 1. Three Na transporters play key roles in cardiac physiology and pathology, Na/K pumps, Na/Ca exchangers, and NHEs. All three appear to be importantly regulated by inactivation reactions that depend on ion binding to transport sites, Na in the case of Na/Ca exchangers and Na/K pumps and possibly both Na and protons in the case of NHEs.

the ATPase activity of the pump, while K binding controls dephosphorylation. Given that two of the most important biochemical reactions of the body are controlled by binding a specific number of Na or K ions in a transport cycle, why would evolution not have put this principle to use to regulate other processes that depend strongly on ion concentrations? As sketched in this Viewpoint, this seems increasingly to be the case, although the structural basis of these regulatory processes remains almost completely unexplored. In the case of NCX1 Na/Ca exchangers and Na/K pumps, inactivation mechanisms clearly depend on achieving specific transporter conformations that can be changed by manipulating the concentrations of ions transported (Hilgemann et al., 1992b; Lu and Hilgemann, 2017). While it is possible, even likely, that additional regulatory molecules become involved, the case for dependence on transport site occupation seems strong. In the case of NHEs, primarily NHE1 and NHE3, the case is less clear, but numerous experimental results to be considered here seem consistent with this interpretation. Similarly for a number of ion channels, it now seems certain that occupation of channel pores by transiting ions can control important channel gating reactions. In other ion channel cases, the working hypothesis of this Viewpoint is presently tantalizing and deserving of more experimental attention, but it remains speculative.

Secondary regulation of Na/Ca exchange by Na-dependent inactivation

Electrophysiologists tend to be very aware of the limitations of their methods and perhaps were overly ready to admit that patch clamp does not decisively control ion concentrations. Therefore, it was widely assumed that ion concentrations were changing when transport currents generated by Na/Ca exchangers and Na/K pumps decayed subsequent to their activation by applying appropriate concentrations of the transported ions. Our first measurements of Na/Ca exchange activity in giant membrane patches, however, revealed immediately that exchangers were subject to inactivation reactions that in some way depended on cytoplasmic Na (Hilgemann, 1990). At least, given the open nature of the giant patch preparation, it was biophysically nearly impossible to explain by other hypotheses why outward exchange current activated by applying 10 to

50 mM cytoplasmic Na in the presence of extracellular Ca would decay substantially, why that decay would be entirely disrupted by protease treatment, and why the current decay would be alleviated by ATP-dependent processes.

Fig. 2 describes, to the best of our present knowledge, how the inactivation reactions control exchange activity (Hilgemann et al., 1992a,b), and Fig. 3 underscores the importance of the Na-dependent inactivation for NCX function and regulation. In brief, the exchanger functions in general by a simple cycle in which three Na are transported inwardly (movement from states 3 to 4) while one Ca is transported outwardly (movement from states 1 to 2) with two Na competing for one Ca at one site (not illustrated) and one Na likely binding at a separate site (Kang and Hilgemann, 2004). After analysis of both forward (Ca extrusion) and reverse (Ca influx) modes of NCX operation with variation of both ions on both membrane sides, we concluded that inactivation must be occurring primarily or nearly exclusively when three Na are bound to the inwardly facing transport sites. This was also supported by whole-cell measurements in which extracellular Na or Ca were both shown to promote inactivation by “pushing” exchangers from the configuration open to the outside to a configuration open to the inside, thereby making exchangers conducive to inactivation in the presence of cytoplasmic Na (Matsuoka and Hilgemann, 1994). The fact that inactivation could be largely ablated by an ATP-dependent process turned out to reflect the ATP-dependent generation of phosphatidylinositol 4,5-bisphosphate (PIP₂; Hilgemann and Ball, 1996), which like other anionic lipids, such as phosphatidate (Hilgemann and Collins, 1992), could prevent the Na-dependent inactivation (i.e., the transition from state 4 to state 5).

At the same time, it became clear that exchangers were activated by a Ca-dependent regulatory mechanism (transitions from states 7 to 4 and 6 to 5) that did not require ATP, and this secondary regulatory mechanism turned out to involve Ca binding to auxiliary sites in the large cytoplasmic loop of the exchanger (Philipson et al., 2002; Hilge et al., 2009; Dixit et al., 2013; Tal et al., 2016). While we could model in first approximation these regulatory processes as occurring in parallel, and in an independent fashion, it appears now much more likely that they are functionally interactive reactions. Binding of Ca to regulatory sites makes Na-dependent inactivation less likely, and Na-dependent inactivation makes activation by Ca less likely. Fig. 3 A illustrates the major regulatory behaviors that were explained, and Fig. 3 B shows simulation results for the refined inactivation model. From left to right in Fig. 3 A, application of high Na to the cytoplasmic side of a giant cardiac patch results in immediate activation of outward current, followed by its decay by ~65% over several seconds. In the absence of cytoplasmic Ca, no current can be activated by cytoplasmic Na. In the presence of cytoplasmic Na, current turns on and off over the course of 3–8 s as cytoplasmic free Ca (2 μM) is applied and removed in well buffered solutions. As shown in the fourth trace, exchangers are fully available when Na is applied and Ca is removed at the same time. When no current is activated by Na in the absence of Ca, currents activate within <1 s when Ca and Na are applied together. This reflects a fast transition from

SODIUM-CALCIUM EXCHANGE

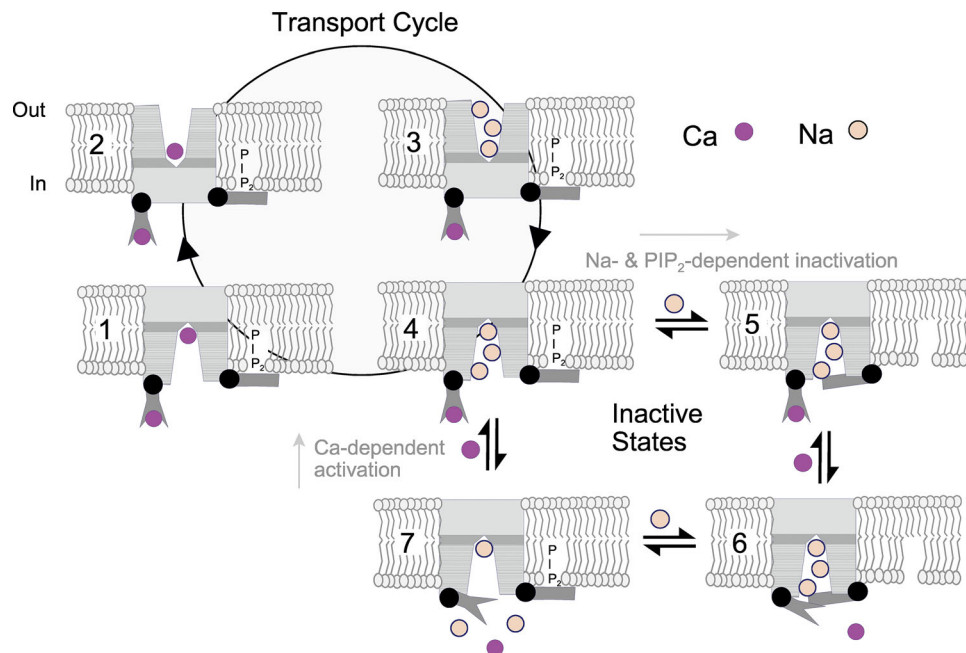


Figure 2. **Ion transport cycle and inactivation reactions of the cardiac (NCX1) Na/Ca exchanger.** The transport cycle (states 1 to 4) moves one Ca outwardly and three Na ions inwardly. Inactivation occurs preferentially when three Na are bound to the inwardly facing transport sites and anionic phospholipids such as PIP₂ are depleted (states 4 to 5). A second inactivation process occurs preferentially when regulatory Ca binding sites are not occupied by Ca (states 4 to 7 and 5 to 6). The two inactivation processes are interactive and reinforce one another.

inactive state 7 to the active cycle, while recovery from the Na-inactivated state 6 takes many seconds.

Using the same parameters as in Fig. 3 B, the Na-dependent inactivation model predicts very well how cytoplasmic ATP and PIP₂ (or other anionic lipids) activate NCX1 and modify its function. Fig. 3 C shows specifically how the steady-state Ca dependence of reverse exchange activity is modified by increasing the rate of Na-dependent inactivation from 0 to 1 s⁻¹. In the absence of regulation by Na binding, exchange current can be very significant at very low free Ca (<10⁻⁸ M), and the exchanger is fully activated by 10⁻⁷ M free Ca. As the Na-dependent inactivation increases, the maximal steady-state exchange current decreases and the half-maximal cytoplasmic free Ca required for secondary activation increases to at least 1 μM. These results mimic well results for ATP activation of cardiac and squid exchangers (Requena, 1978), and they mimic well observations for activation by anionic lipids, consistent with the hypothesis that the “inactivation gate” of the exchanger, likely the cationic PIP₂-binding domain dubbed “XIP domain,” may physically bind anionic lipids and thereby be pulled away from an inhibitory position that also promotes inactivation by domains coupled to the regulatory Ca sites (Matsuoka et al., 1993).

What is the physiological sense of Na-dependent inactivation of Na/Ca exchangers? One possibility stems from the fact that Na/Ca exchangers cannot establish a Ca gradient when cytoplasmic Na rises excessively. It then becomes a mediator of cardiac myocyte demise. The Na-dependent inactivation may at least in part prevent this pathological function, and it should soon be possible to test this hypothesis in animal models

expressing exchangers with modified inactivation. It also remains to be determined whether the Na-dependent inactivation inhibits transport activity by blocking specific conformational changes of the transport cycle or whether all ion transport reactions (Kang et al., 2003) are affected.

Secondary regulation of Na/K pumps by Na-dependent activation

For decades, cardiac physiologists have proposed that cytoplasmic Na can accumulate in subsarcolemmal microdomains where such accumulations may play major signaling roles by locally controlling Na/Ca exchange function and/or the function of other transporters (Lederer et al., 1990; Carmeliet, 1992; Wendt-Gallitelli et al., 1993; Chu et al., 2019). In recent work, we attempted to evaluate this hypothesis by measuring subsarcolemmal Na via Na current reversal potentials and evaluating the turnover times of all monovalent ions in cardiac myocytes (Lu et al., 2016; Lu and Hilgemann, 2017). It exceeds the scope of this review to reiterate the different types of evidence employed to test this hypothesis and our arguments against the hypothesis. Suffice it here to summarize that only one biophysical mechanism has been proposed to explain how Na diffusion over distances of ≤1 μm could take multiple seconds. Carmeliet evoked the existence of “structured water” (Carmeliet, 1992) as proposed earlier by Ling, 1965 to explain the extraordinary restriction of Na diffusion required to explain Na/K pump current decay during pump activation by K.

As just implied, one key observation used to support the local Na hypothesis is that Na/K pump currents often decay markedly during their activation by extracellular K over a timescale of a

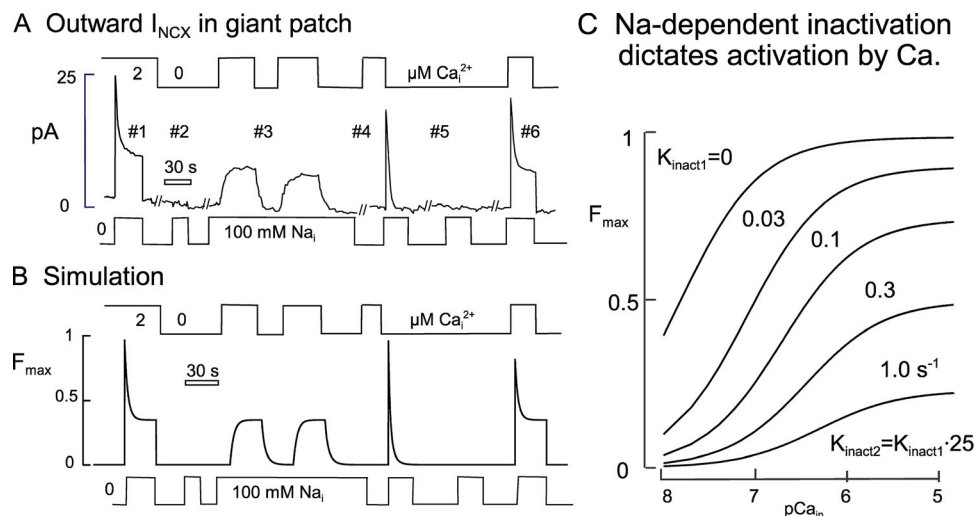


Figure 3. Simulation of the two parallel NCX1 inactivation reactions revealed in studies of cardiac giant membrane patches. (A) Exchange currents recorded after step changes of cytoplasmic Na and Ca. From left to right: (1) When exchange current is activated by a step increase of cytoplasmic Na (100 mM) in the presence of cytoplasmic Ca (2 μ M), exchange currents decay by 10 to >90% with a tau of several seconds. (2) In the absence of cytoplasmic Ca, no current is activated by application of Na. (3) In the presence of Na, outward exchange current turns on and off with a tau of \sim 8 s when cytoplasmic Ca is applied and removed. (4) When Na is applied and Ca is removed simultaneously, current decays to negligible values with a multisecond time course. (5) Na application without Ca activates no current. (6) However, simultaneous application of Na and Ca after a period of no Na/no Ca activates the peak exchange current, reflecting a fast transition from state 7 to 4 in the diagram of Fig. 2. **(B)** Simulation of the same exchange current function. **(C)** Effect of increasing solely the rates of the two Na-dependent inactivation processes in parallel (i.e., transitions 4 to 5 and 7 to 6). The changes that occur for Ca regulation include both a shift of the half-maximal Ca to higher concentrations and a decrease of the maximal exchange current observed. The rightward shifts of these curves correspond well to the observed effects of deleting ATP and/or anionic phospholipids from patches, while the leftward shifts correspond well to effects of increasing anionic phospholipids. This includes the development of high exchange activity at extremely low free Ca.

few seconds, much too pronounced and too fast to reflect bulk changes of cytoplasmic Na. Rather than reflecting local Na depletion, as would be expected from Fig. 1, our work is much more consistent with an alternative idea that rapid pump current decay reflects mostly a secondary inactivation of Na/K pumps by principles similar to those just outlined for Na/Ca exchangers. In distinct contrast to Na/Ca exchangers, however, a rise of cytoplasmic Na favors pump activation, and Na deficiency favors pump inactivation (Lu and Hilgemann, 2017).

Fig. 4 summarizes in cartoon form the Na/K pump cycle and the function of inactivation reactions as suggested by our recent studies. The Post-Albers Na/K pump cycle scheme (Skou, 1998) is well known to readers of this journal; pumps with binding sites open to the cytoplasmic side are called E_1 states, while pumps open to the extracellular side are called E_2 pumps. When the pump has bound three Na on the cytoplasmic side (state 1), it phosphorylates itself and occludes the three Na ions (state 2). Upon opening to the outside (state 3), the Na ions are released and two K bind (state 4), followed by dephosphorylation and opening to the cytoplasmic side (state 5) with release of K into the cytoplasm. Na/K pump inactivation becomes stronger as the cytoplasmic Na concentration is reduced, and the inactivation can often, but not always, be suppressed by increasing cytoplasmic Na. Accordingly, we suggested that pumps tend to inactivate (state 5 to state 6 transition) when they are oriented to the cytoplasmic side (i.e., in E_1 configuration) and their binding sites are not fully occupied by Na. We cannot exclude a possibility that cytoplasmic K binding may contribute to inactivation by forcing pumps backward in the cycle into stable K-occluded

states, but cytoplasmic K is with good certainly not required for inactivation (Lu et al., 2016).

Since Na/K pump inactivation does not usually occur when pumps are studied in excised giant patches, we entertain the idea that inactivation may involve the binding of an endogenous inhibitor (“X” in state 6) either to the phosphate coordinating site or to transport sites. That such a molecule exists is strikingly supported by the observation that pump currents turn on slowly over several seconds in giant excised patches on the first application of cytoplasmic ATP and thereafter remain irreversibly and highly activated (Friedrich et al., 1996; Hilgemann, 1997). In any case, it is apparent that recovery from inactivation is dependent on binding cytoplasmic Na and likely requires that all three Na sites are occupied (see transitions from states 6 to 7 to 1).

To summarize our proposal, Na/K pumps undergo inactivation that can be called Na-deficiency inactivation with recovery by a Na-promoted mechanism. The physiological “sense” of this regulatory process is that cells will maintain a substantial fraction of their pumps as a pump reserve in an inactive state that can be recruited for active transport as needed when cytoplasmic Na begins to rise. The inactivation mechanism remains pronounced, but is less strong, in myocytes that lack the “gamma subunit” of Na/K pumps in muscle, phospholemman (Lu et al., 2016). In this light, it would be of great interest to know whether other FXD proteins might support Na/K pump inactivation and whether they might become more important in phospholemman-knockout mice.

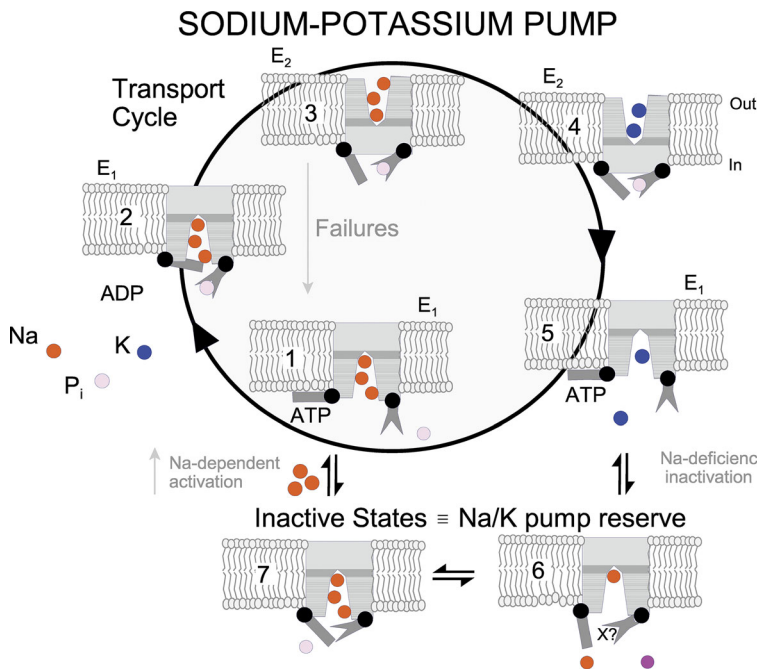


Figure 4. Post-Abers Na/K pump cycle with suggested in-activation reactions. When three Na are bound to pumps with inwardly facing binding sites (E₁, state 1), pumps phosphorylate themselves and occlude Na (state 2), followed by opening to the outside (E₂, state 3), release of Na and binding of 2 K (state 4), dephosphorylation with opening to the inside and release of K (state 5), and rebinding of cytoplasmic Na. Pumps appear to inactivate from E₁ states in which Na-binding sites are not fully occupied (states 5 to 6), and recovery from inactivation occurs primarily when binding sites are loaded with Na (states 7 to 1). It is speculated that a small molecule could mediate inactivation by interacting with the phosphorylation site of functionally associated sites ("X" in state 6). It is assumed in simulations that pump failures can occur in which pumps in E₂ configuration with three Na loaded dephosphorylate and return to the E₁ state, thereby returning three Na to the cytoplasm without completing a pump cycle. Alternatively, ADP may accumulate significantly in isolated myocytes and allow backward movement of three Na with synthesis of ATP. In either case, the slippage caused by such "failures" becomes negligible in the presence of extracellular K.

That the secondary Na-dependent regulation of Na/K pumps is connected to extrinsic regulatory mechanisms is illustrated in Fig. 5. As shown in Fig. 5, A and B, we studied Na/K pump function in mouse myocytes using half-maximal cytoplasmic Na concentrations and attempted to identify factors that might regulate pump activity. Surprisingly, from many classical signaling mechanisms examined, we found that in mouse

myocytes, cytoplasmic Ca elevation caused the largest regulatory increases of Na/K pump activity (Lu et al., 2016). Fig. 5 B shows a typical experiment in which Na/K pump currents were activated by applying repeatedly 7 mM extracellular K for 12 s followed by a 1-min pause. The pump current decays by ~70% during the initial two applications of K. When Ca was then applied for 5 s, reverse Na/Ca exchange current turns on over a

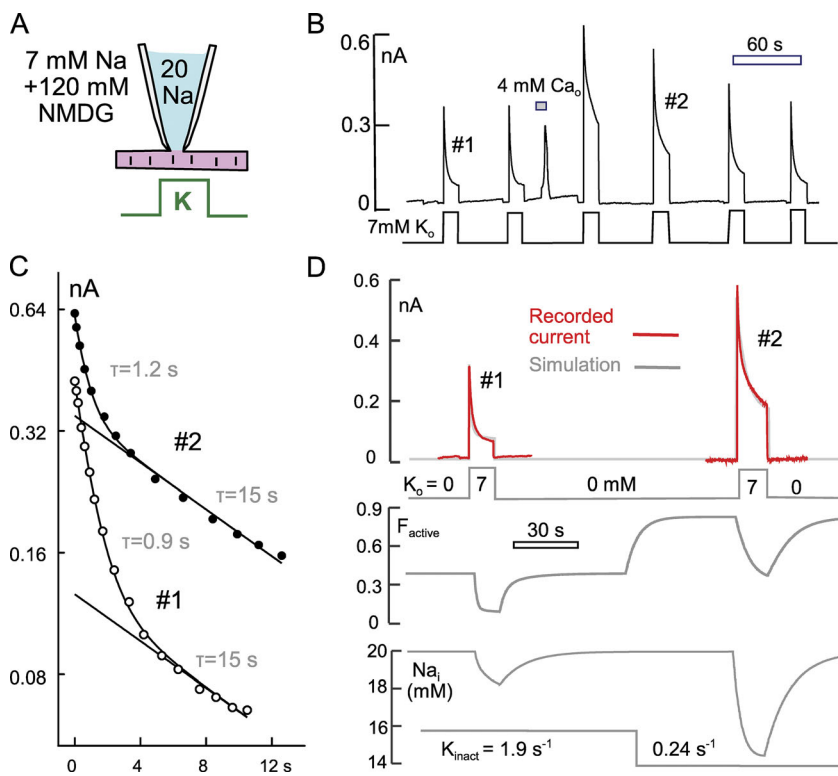


Figure 5. Na/K pump currents in a mouse myocyte, recorded as described previously (Lu et al., 2016). (A) Whole-cell recording of pump current with 20 mM cytoplasmic Na and 7 mM extracellular Na. (B) Pump current is activated six times by application of 7 mM K for 12 s in exchange for 7 mM Na. After the second application of K, cytoplasmic Ca (4 mM) is applied for 5 s, and reverse exchange current is activated, resulting in spontaneous myocyte beating for ~10 s (not illustrated). Thereafter, peak pump current is increased ~70%, pump current at 12 s is increased more than threefold, and current decay is decreased substantially. The stimulatory effects reverse completely within 2 min. (C) Semi-log plot of Na/K pump current decay before (1) and after (2) Ca application. Decay shows fast and slow components with time constants of ~1.2 and 15 s. The fast component becomes smaller and the slow component becomes larger after Ca application. The slow component reflects Na exchange between the cytoplasm and the pipette tip. (D) Simulation of the model from Fig. 4. "F_{active}" is the fraction of pumps in the active state. To simulate the effect of Ca, the inactivation rate constant is decreased with no other parameter changes. Peak currents increase because pump failures promote accumulation of inactive pumps in the absence of extracellular K. Larger pump currents after decreasing inactivation result in greater depletion of cytoplasmic Na (see predicted cytoplasmic Na concentration). Predicted Na/K pump current match well the measured Na/K pump current transients.

few seconds as cytoplasmic Ca rises and activates the exchanger via the mechanisms outlined in Fig. 2. Thereafter, peak pump currents are increased by about twofold, and the pump current occurring after 10 s is increased three- or fourfold. Subsequently, pump currents decrease back to baseline levels over 2 min.

Fig. 5 C shows semilogarithmic plots of the current decay from records 1 and 2 (i.e., before and after Ca elevation) after subtraction of an asymptote. The current decay shows two components. A fast component decays with a time constant of ~ 1 s, and a slow component decays with a time constant of ~ 15 s. The latter, slower component corresponds well to our estimate of monovalent ion equilibration with the pipette tip in these experiments. The former, smaller time constant corresponds to the major inactivation reaction. As apparent in Fig. 5 C, the decay component with the slower time constant becomes much larger when pump activity is stimulated, corresponding presumably to a larger depletion of bulk cytoplasmic Na. The decay phase with the small time constant becomes smaller with increased pump activity, indicating that pump currents may be enhanced primarily by alleviating the inactivation process.

Simulations shown in Fig. 5 D lend further credence to this interpretation. To re-create the experimental results, Na exchange between the cytoplasm of a myocyte and the pipette tip is simulated to take place with a 15-s time constant with the pipette containing 20 mM Na. This time constant is roughly as expected for free diffusion from simulations of a pipette tip with an access resistance of 3 M Ω and communing to the cytoplasm of a myocyte with a mixing volume of 11 pl (Lu and Hilgemann, 2017). The pump cycle was simulated essentially as outlined in Fig. 4 with inactivation occurring to a single inactive state from pumps in the E₁ state (i.e., open to the cytoplasm) with at least one unoccupied Na-binding site. Recovery was simulated to occur from inactive states with three Na bound.

With these assumptions, a decrease of the inactivation rate reproduces well the change of shape of the Na/K pump current decay after a Ca elevation. However, peak pump current during application of extracellular K does not increase in simulations if all pumps are in the E₂ configuration in the absence of extracellular K. To account for the increase of peak pump current, one might assume that pumps can indeed inactivate to some extent from E₂ states. It is, however, unlikely that all pumps are in the E₂ state in the absence of K. Nearly all ATP-driven ion pumps undergo “slippage” in certain circumstances (Inesi and Tadini-Buoninsegni, 2014), and Na/K pumps can likely undergo “failures” by multiple mechanisms in the absence of extracellular K (Glynn and Karlish, 1976). In the simulation presented, it is assumed that three Na can occasionally be transported back to the cytoplasmic side in the absence of extracellular K (and cytoplasmic ADP), accompanied by dephosphorylation. Pump failures of this type appear to occur in some, but not all, cell types (Blostein and Mallet, 1995). They are functionally equivalent to effects of ADP accumulation in the simulation model (step 13 of the Na/K pump model employed), which might also occur in isolated cardiac myocytes. With the assumption of either genuine pump failures or significant ADP accumulation in myocytes, the effects of Ca elevation are accounted for accurately by

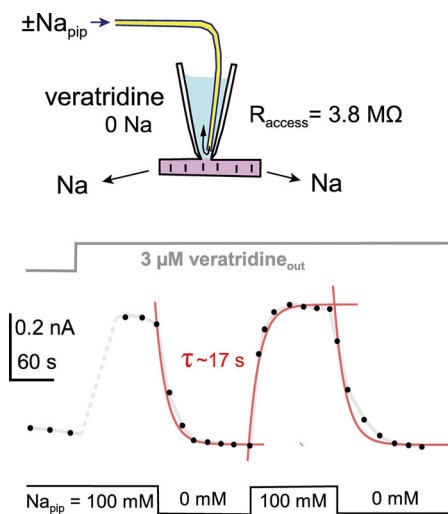


Figure 6. **Rapid pipette perfusion (Hilgemann and Lu, 1998) to determine the time course of cytoplasmic Na exchange with the pipette tip.** Experimental conditions were as described previously (Lu and Hilgemann, 2017), and myocytes were made permeable to monovalent cations with veratridine (3 μ M). Using Na as the sole permeable cation, 100 mM Na was exchanged for 100 mM NMDG in the pipette tip. The veratridine-activated outward current decays with a time constant of 17 s upon removing Na from the pipette tip and is restored upon reintroduction of Na with a time constant of 17 s. The fact that current decays somewhat below baseline upon removing Na reflects the existence of a small myocyte Na conductance in the absence of veratridine. Experiments reveal no slow components of Na exchange or evidence for local, subsarcolemmal Na depletion/accumulation.

decreasing the inactivation rate. Importantly, the occurrence of failures becomes negligible in the presence of extracellular K and would be of no real physiological consequence.

As shown in Fig. 5 D, reduction of the rate of inactivation from 1.9 to 0.24 s⁻¹ doubles the number of active pumps (see middle trace), and the increased pump activity then causes a larger depletion of bulk cytoplasmic Na during pump activity. Whereas the pump current decay is largely due to inactivation in response 1, which is represented by a larger fast component, pump current decay in response 2 is largely due to depletion of bulk cytoplasmic Na, which decreases from 20 to <15 mM. In summary, Na depletion remains small in the control response 1 because pumps inactivate, while Na depletion with a time constant of ~ 15 s occurs throughout the cytoplasm with no local Na gradients after inactivation has been removed.

That Na indeed turns over from the pipette tip to cytoplasmic face of the myocyte sarcolemma with a time constant of ~ 15 s is illustrated in Fig. 6. Using a rapid pipette perfusion technique, as described previously (Hilgemann and Lu, 1998), we employed myocytes made permeable to monovalent cations by treating them with veratridine to measure directly ion turnover from the pipette tip. NMDG was used as the sole monovalent cation on the outside, and the pipette solution contained initially 100 mM Na with 40 mM NMDG. Application of veratridine then activates an outward Na current of ~ 0.5 nA. Upon perfusing Na out of the pipette tip by applying positive pressure to a solution reservoir containing 140 mM n-methyl-d-glucamine with no Na, the outward Na current decays with a time constant of 17 s, and the

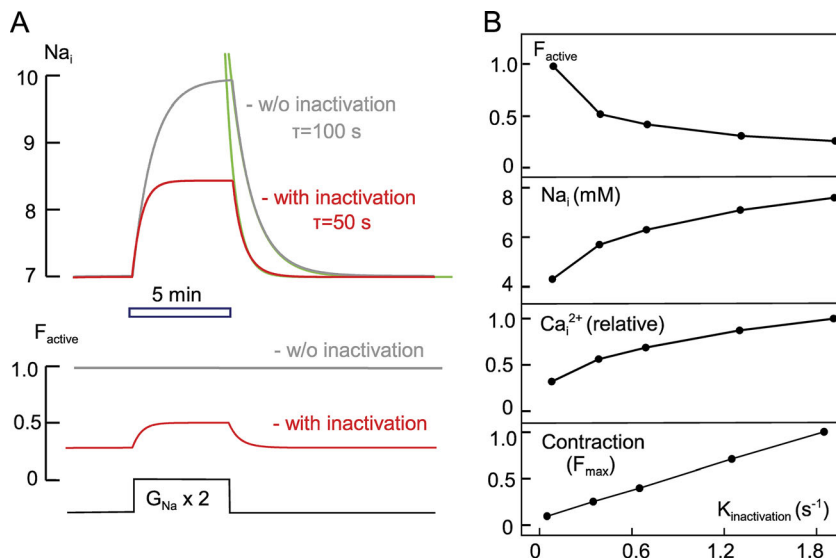


Figure 7. Simulation of Na/K pump function in an intact cell with and without inactivation that generates a pump reserve three times larger than the active pump pool with 7 mM cytoplasmic Na. **(A)** Simulated cytoplasmic Na changes with and without inactivation. As indicated, a background Na current of 47 pA was doubled to 94 pA in the simulation for 5 min and then decreased again to 47 pA. Na-dependent recovery from inactivation blunts the increase of Na by 50% and doubles the apparent speed with which Na homeostasis occurs. Na homeostasis occurs nearly exponentially with a time constant that is substantially smaller than the average dwell time of Na ions in the cell. **(B)** Predicted physiological implications of regulated Na/K pump inactivation for cardiac myocytes. As the inactivation rate increases from negligible values to 1.8 s^{-1} , 65% of Na/K pumps inactivate, consistent with pump currents described in Fig. 5 (top graph). This degree of inactivation causes a doubling of cytoplasmic Na from 4 to 8 mM (second graph), which would in turn cause a nearly fourfold increase of the cardiac Ca transient (third graph). Assuming a C–force relationship with a Hill slope of 2.7, these Ca changes translate to contraction changes over the full range of cardiac contractility (bottom graph). More details for cardiac ECC are outlined in a separate article (Hilgemann, 2019).

current can be reversibly restored with a very similar time constant. As expected, this time constant is essentially the same as the time constant of ion exchange determined by varying extracellular ion concentrations in patch-clamped myocytes in the presence of large membrane conductances (Lu and Hilgemann, 2017). Neither these experiments nor other tests for the existence of slowly exchanging Na compartments (e.g., equivalent pipette perfusion experiments using Na/K pumps to sense submembrane Na concentration changes; Hilgemann, 2019) give any evidence in our hands for the existence of restricted subsarcolemmal Na spaces. The time constant of Na exchange is the same when determined via variation of Na influx through ion channels or variation of Na in the patch pipette tip.

The potential physiological importance of Na-dependent secondary regulation of Na/K pumps is illustrated for cardiac muscle by simulations in Fig. 7. The consequences for Na turnover in myocytes are elaborated in Fig. 7 A via simulations of a cardiac myocyte without patch clamp in the presence of a continuous background Na channel influx. In one simulation, Na/K pump densities were assumed as in the patch-clamped mouse myocyte, and the inactivation mechanism was adjusted so that two thirds of pumps inactivated in the steady state in the presence of 7 mM Na. In a second simulation, Na/K pumps were simulated without inactivation, and the total number of pumps was reduced by two thirds to give the same pump current at 7 mM Na. Then, as indicated in Fig. 7 A, the background Na conductance was doubled for 5 min. The benefit of having a pump reserve is that recruitment of pumps occurs as Na rises and promotes Na homeostasis to develop more rapidly. The second benefit is that the threefold pump reserve blunts Na accumulation by one half and reduces the time constant of Na homeostasis from 180 to 90 s.

In summary, the Na/K pump inactivation mechanism has obvious homeostatic benefits for cells in controlling the influence of Na flux changes on Na-dependent cell processes, such as Ca homeostasis. Regulation of the inactivation mechanism by cell signaling processes can allow myocytes to switch between states in which cytoplasmic Ca is dependent on Na influx to a greater or lesser extent. Fig. 7 B summarizes the expected effects of increasing Na/K pump inactivation from a negligible rate up to an extent that 65% of pumps are inactive. From top to bottom in Fig. 7 B, the active fraction of pumps decreases from 1 to 0.35, cytoplasmic Na increases from 4 to 8 mM, in a simple model of cardiac excitation–contraction coupling with a 3-to-1 Na/Ca exchanger, a doubling of cytoplasmic Na will cause a fourfold increase of the Ca transient, and as a result of the steep relation between Ca and force development (Hill slope >3 , possibly as high as 5; Backx et al., 1995; Dobrunz et al., 1995), the expected Ca transient changes could result in contraction changes that encompass 90% of the contractile range of a myocyte. The prediction shown in the bottom panel of Fig. 7 C employed a Hill coefficient of only 2.7 for the Ca–force relation. The physiological relevance of Na/K pump inactivation for cardiac excitation–contraction coupling (ECC) is considered in more detail in a separate article (Hilgemann, 2019).

Secondary regulation of NHEs by protons and Na

The inactivation mechanisms suggested for Na/Ca exchange and Na/K pumps are supported by a wide range of experiments with variation of ions on both membrane sides and tests of different transport/inactivation models in simulations. Unfortunately, the databases and detailed kinetic experiments available for electrogenic transporters are simply not available for other Na transporters, such as NHEs. Nevertheless, many “hints” exist that similar principles do apply to other transporters, and it is

SODIUM-HYDROGEN EXCHANGE

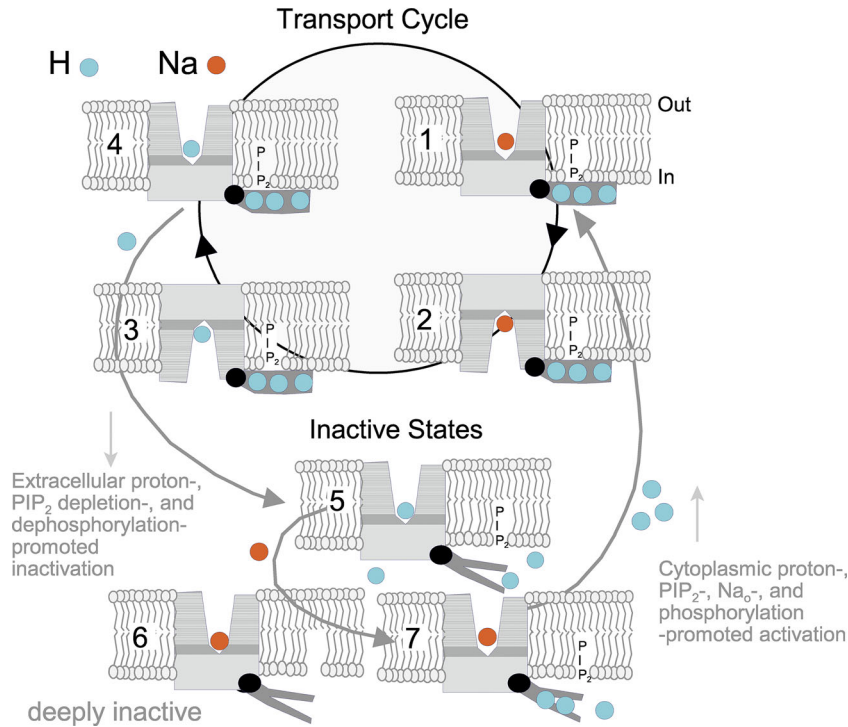


Figure 8. NHE1 Na/H exchange cycle with inactivation. The exchange cycle moves one Na inwardly and one proton outwardly (states 1 to 4) when the exchanger inactivation domain is disengaged and has three protons occluded within it. Exchangers transition to inactivated states with release of regulatory protons preferentially when exchangers are open to the outside and have bound a proton, as well as when anionic lipids such as PIP₂ are depleted from the cytoplasmic monolayer. Inactive states are stabilized by dephosphorylation and loss of protons from regulatory sites. Na binding from either membrane side may favor return to the active states, together with phosphorylation and increased anionic lipid content of the cytoplasmic monolayer.

described here how the Na/H exchange cycle may speculatively be coupled to similar inactivation reactions.

For decades, it has been known that NHEs in the surface membrane of cells, primarily NHE1 and NHE3, are regulated by cytoplasmic pH such that proton extrusion is activated secondarily in a very “steep” fashion as pH falls below 7.0 (Aronson et al., 1982; Wakabayashi et al., 2003). It is also well established that this cytoplasmic proton-dependent activation of exchangers is modified by a number of signaling pathways, such that the proton dependence of exchange activity shifts to a higher pH range as an NHE activation mechanism, and conversely shifts to a more acidic range when ATP is depleted (Grinstein et al., 1985; Bastié and Williams, 1990; Wakabayashi et al., 2003). Similar to Na/Ca exchangers (Hilgemann and Ball, 1996), the inhibition by ATP depletion may reflect a loss of PIP₂ (Aharonovitz et al., 1999, 2000) and/or other ATP-dependent anionic phospholipids, phosphatidate being the primary candidate.

Fig. 8 illustrates a simple scheme that can account for many of the regulatory effects on NHE1, including the possibility raised here that transitions to and from inactive states depend on occupation of transport sites. The normal forward exchange cycle moves one Na inwardly (states 1 to 2) and one proton outwardly (states 3 to 4). All of the active exchanger states can be assumed to have three protons occluded into regulatory sites. When exchangers inactivate (e.g., when PIP₂ decreases), the inactivation domain can be assumed to relax and allow release of the occluded protons from inactive states (states 5–7). A variety of regulatory influences may stabilize more the active or inactive states. These regulatory mechanisms include most prominently exchanger phosphorylation by mitogen-activated protein

kinases that are in turn under control of protein kinase Cs that activate especially the NHE1 isoform (Bianchini et al., 1997).

Fig. 9 illustrates simulations of this scheme that recreate reasonably major NHE regulatory mechanisms described to date. Fig. 9 A shows the predicted pH dependence of forward NHE1 activity and the shift of the activation curve to a more acidic range with ATP depletion, as described by Wakabayashi et al. (2003). Note that the activation by protons becomes steeper after ATP depletion. In the control conditions, the transition from inactive to active states occurs mostly in a higher pH range than the proton dependence of transport, per se. After ATP depletion, the proton dependence of exchange activity reflects largely the secondary activation process. Fig. 9 B illustrates one of many examples of the activation of NHE1 by hormones, namely by gastrointestinal peptides in AR42J cells (Bastié and Williams, 1990), resulting in a shift of pH dependence to a higher pH range. Whereas the former result can be accounted for in our scheme by a loss of PIP₂ with more pronounced inactivation, the latter effect of activating hormones is accounted for simply by a decreased rate of inactivation with no change of the intrinsic proton affinity of the exchanger’s regulatory domain.

Two further results illustrate how the inactivation reactions may be coupled to ion binding to transport sites. Decades ago, the Lazdunski group studied the activation of NHE1 activity in synaptosomes by cytoplasmic acidification (Jean et al., 1985). Remarkably, they found that the activation by cytoplasmic acidification could be countered over at least one pH unit by acidification of the extracellular side. Of course, inhibition by extracellular protons might reflect inhibition by proton competition with Na, but the parallel shifts of cytoplasmic proton activation cannot be explained by that mechanism. Fig. 9 C

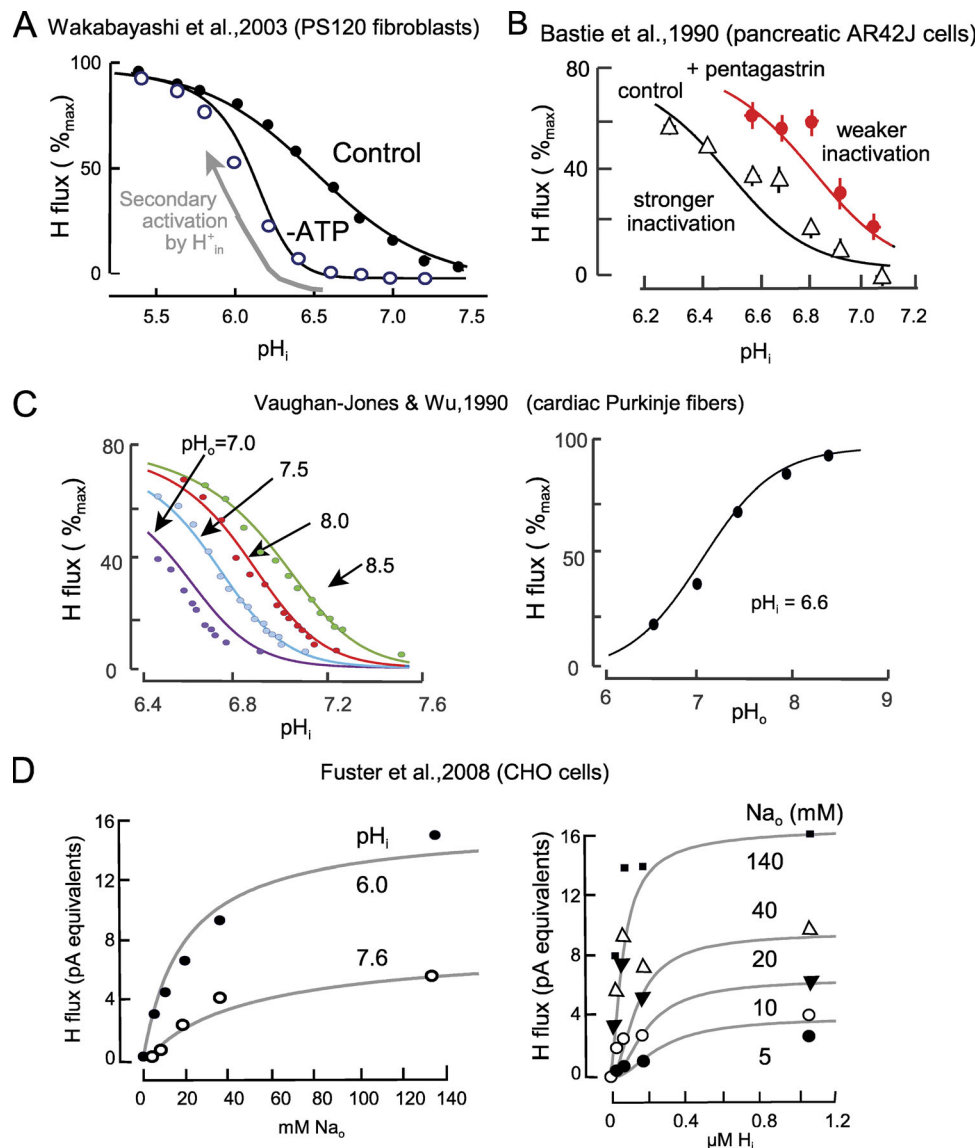


Figure 9. **Simulations of NHE1 Na/H exchange function using the model described in Fig. 8.** Data from the cited papers was extracted digitally and fits were generated as described in the supplemental material. **(A)** Depletion of ATP is assumed to deplete anionic lipids that maintain NHE1 in an active state, thereby favoring inactivation and deocclusion or protons bound to regulatory sites (states 5 to 7 in Fig. 8). Proton dependence reflects mostly binding to transport sites in the control condition, although a 0.3 log unit shift to higher pH is still possible. When ATP is depleted, NHE1 inactivation shifts the secondary activation to a lower pH range so that secondary activation by protons dominates the activation curve. **(B)** Agonists such as pentagastrin in the AR42J pancreatic cell line promote the transitions to active states with occluded protons and shift the activation curve to a higher pH range. **(C)** The left panel illustrates that in cardiac Purkinje fibers acidification of the extracellular solution shifts the activation of NHE activity by cytoplasmic protons to a lower pH range (Hill slope 3.2). These shifts are recreated by assuming that inactivation of NHE activity occurs preferentially when extracellular transport sites are occupied by protons. The right panel shows that the inhibition of NHE1 activity by extracellular acidification follows simple Michaelis–Menten kinetics. **(D)** The left panel shows that in CHO cells activation of NHE1 activity by extracellular Na occurs with a Hill slope of 1 when the cytoplasm is acidic and exchangers are saturated with protons. The Hill slope increases to 2 when cytoplasmic pH is increased. The steeper Na concentration dependence, when cytoplasmic protons are not saturating, reflects a shift of NHE transporters from inactive to active states when transport sites are Na-occupied, thereby stabilizing active transport configurations. The right graph in D shows a more complete dataset for activation of NHE activity by cytoplasmic acidification in a linear plot. Decreasing extracellular Na shifts the activation by protons to a higher concentration range and reveals cooperativity of the proton activation, as lower extracellular Na favors occupation of inactive states.

illustrates the same regulatory principle as it was characterized by the Vaughan-Jones group in cardiac Purkinje fibers (Vaughan-Jones and Wu, 1990). In these experiments, the cytoplasmic pH dependence of normal forward exchange activity was determined at four different extracellular pH values with a normal Na gradient. As extracellular pH is decreased, the steep

activation by cytoplasmic acidification (Hill coefficient, 3.2) shifts to a progressively lower pH range. As shown in the right panel, the inhibition of NHE activity by extracellular acidification in the presence of a nearly maximal cytoplasmic proton concentration (pH 6.6) occurs with a simple inverse Michaelis–Menten form, as expected for simple competition

between Na and protons at transport sites. To explain the shifting of the cytoplasmic activation curve by progressive extracellular acidification, it is assumed in this simulation that inactivation occurs preferentially when extracellularly oriented transport sites for protons are occupied. The rapid reversibility of the extracellular proton effects in these experiments, as well as in the synaptosome experiments, is at least very consistent with this transport-site interpretation.

A second case where transport sites may affect the distribution of NHE exchangers between active and inactive states relates to the activation of exchange activity by Na, both forward mode and reverse modes. In studying NHE1 activity in a variety of patch-clamped cells, we found that as the cytoplasmic pH was increased (i.e., proton concentration decreased), the activation curve for extracellular Na became steeper and reached typically a Hill slope of 2 (Fuster et al., 2008). This is illustrated in the left panel of Fig. 9 D, while the right panel shows the available datasets plotting the cytoplasmic proton concentration dependence of forward exchange at different extracellular Na concentrations. At the time of these experiments, we were impressed that these and other complex results could not be explained by any simple transport model. We assumed further at that time that a Hill coefficient of 2 indicated that at least two Na-binding sites must be involved in the activation curve for Na at low intracellular proton concentrations. In this light, we interpreted the datasets in the context of functional dimer models in which the binding of Na by one transporter could influence binding by the second transporter in the dimer. A great insecurity about any of the models was underscored by the fact that the databases could be reasonably accounted for by two very different dimer models.

The interpretation of these data in terms of two Na-binding sites presupposed that Hill slopes of 2 are indicative of two binding sites. An alternative that arises from the model of Fig. 8 is that transitions from inactive states to active states might be promoted by Na binding in a manner that is homologous to recovery from inactivation in Na pumps. In this scenario, Na binding within inactive states of NHEs would overcome inactivation caused by high cytoplasmic pH and low extracellular pH. When cytoplasmic pH is relatively high, the Na dependence of forward transport gains a steeper dependence on Na as Na promotes recovery from inactivation and active transport. When cytoplasmic pH is low, the exchangers are preactivated via the proton regulatory sites, and the Na dependence observed in experiments reflects only Na binding by transport sites engaged in transport. The tendency of exchangers to inactivate in the presence of low Na applies also to the cytoplasmic side, giving rise to steep Na dependence also for reverse transport (Green et al., 1988). Whether this mechanism, if it is correct, has real physiological significance is not at all clear. It would certainly not be surprising that the occupation of Na transport sites stabilizes transport-competent conformational states of ion transporters, and this simple physical principle might well have catalyzed evolution of inactivation mechanisms of true physiological import.

In summary, the old adage taught to many of us was that a Hill slope indicates the least number of binding sites that can

underlie a biological process. In other words, a Hill slope of 2 indicates that at least two binding sites are involved. This need not be the case. One can readily construct cases in which the Hill slope is large but only one ion-binding site is involved. For example, imagine an ion channel activated by a Ca-dependent protein kinase that binds only one Ca ion. Nevertheless, the channel may need to be phosphorylated at multiple sites to open. Ca dependence of channel openings will be steep, although only one Ca binding site is involved. The present case may be similar. In the inactive state, Na binding to transport sites may promote recovery from inactivation that gives rise to a steep Na dependence, because Na is also required for transport. Of course, the Na affinities may be different for recovery from inactivation and transport. Still, a single binding site may give rise to the Hill slope of 2.

Before leaving Na/H exchange, one more example of NHE regulation by Na has long been deserving of further attention. As discussed subsequently, ENaCs undergo gating changes in dependence on both extracellular and cytoplasmic Na. Following up on experiments showing inactivation of ENaC activity by a rise of cytoplasmic Na, the Cook group found that Na/H exchange in salivary glands was also subject to long-term inactivation in response to a rise of cytoplasmic Na (Ishibashi et al., 1999). Impressively, these authors found that this response was mediated by, or required, the activity of a pertussis toxin-sensitive G protein, and we verified these results using Chinese hamster ovary (CHO) cells (Hilgemann et al., 2006). Whether this Na-dependent inactivation process reflects the operation of a Na sensor separate from the NHE, i.e., a G-protein regulated by Na binding (Ash et al., 2012), or whether it reflects a regulatory process that interacts with Na-bound transport sites remains unknown. Furthermore, it remains unknown what G protein is engaged in this inactivation process, even though multiple G proteins have been determined to interact with and modify NHE1 function (Hooley et al., 1996; Lin et al., 1996, 2003).

Epithelial Na channels (ENaCs)

Progress in elucidating how electrical signaling occurs in excitable cells relied heavily upon the idea that ion channel gating occurs independently from ion channel permeation. While this notion has served the field admirably, the number of cases in which this simple separation of mechanisms becomes blurred has grown substantially. One of the first and most profound examples of ion channels modifying their conductance in response to Na concentration changes appeared in 1977. In a study using the classical frog skin epithelium preparation, Fuchs et al. (1977) described that ENaCs undergo autoinhibitory responses when extracellular Na is increased, and it was later described that ENaCs also undergo autoinhibition when Na is increased stepwise on the cytoplasmic side (Abriel and Horisberger, 1999). In addition, proton binding to extracellular sites in the channel pore strongly influences channel activity. These autoregulatory phenomena in ENaCs, mediated by extracellular Na and protons (Chraïbi and Horisberger, 2002), have been determined to occur at sites in an extracellular cleft of the channel that are close to, but likely not identical to, the immediate sites of Na permeation (Collier et al., 2014; Kashlan et al., 2015). The inactivation of

ENaC activity that occurs with a rise of cytoplasmic Na (Dinudom et al., 1998; Abriel and Horisberger, 1999) remains more enigmatic, as it appears to require the presence of soluble factors that can be lost over time in “cut-open” oocyte recordings (Abriel and Horisberger, 1999). In this sense, the cytoplasmic Na-dependent inactivation of ENaCs is similar to Na/K pump regulation that appears to be lost in excised membrane patches (Friedrich et al., 1996; Hilgemann, 1997). Whether Na binding in the cytoplasmic pore of ENaCs may play a role or whether separate Na-sensing signaling molecules are involved remains unknown. In any case, the possibility exists that the same still-unknown regulatory molecules influence the function of ENaCs, Na/H exchange, and Na/K pumps. Twenty years have now passed since these fundamental observations were reported. Obviously, a resolution of the underlying enigmas can bring major new insights to the Na transport field.

Other ion channels

It would far exceed the scope of this Viewpoint to review the many cases in which ion channel gating can be modified by ion binding in the channel pores. Suffice it here to note three examples in which pore-dependent gating occurs and is likely of substantial physiological significance. The strong inward-rectifier K channels are long known to be increasingly activated as extracellular K rises, and this activation phenomenon has been shown to be physiologically important in several tissues (e.g., to hyperpolarize endothelial cells when small increases of extracellular K occur; Jackson, 2017). While this activation has traditionally been ascribed to interactions between extracellular K binding and cytoplasmic polyamine block, much of the effect has been ascribed more recently to pore blockade by external Na (Ishihara, 2018). It is at least a valid question whether signaling proteins and other ion channels that may interact with strong inward rectifiers might be affected by conformational changes mediated by extracellular K changes.

As second example, the two-pore K channels are strongly outwardly rectifying potassium channels, and their depolarization-dependent activation has recently been shown to rely on movement of cytoplasmic K ions into the selectivity filter, a mechanism that can well be characterized as an “ion flux-gated” mechanism of activation (Schewe et al., 2016). As third example, the diverse class of chloride (Cl) channels dubbed “CLC” channels, and exemplified by the CLC channel cloned from Torpedo electric organ, show remarkable gating changes in response to Cl concentration changes, likely relying on a Cl activation site that is located within the channel pore (Chen and Miller, 1996; Chen, 2003). Notably, the opening rate constant is highly sensitive to extracellular Cl, while the closing rate is more sensitive to cytoplasmic Cl. The major “physiological” outcome is that Cl-dependent gating shifts channel opening to more negative potentials as extracellular Cl increases. However, the in situ physiological roles that Cl-dependent CLC gating may play remain largely unknown and are likely to be a rich area of future research, given that CLCs play critical roles both in the surface membrane and in many different internal membrane compartments of mammalian cells (Jentsch and Pusch, 2018). In summary, it is clear that ion binding within ion channel pores

plays a central role in the gating of many ion channels and that this type of ion pore gating will be relevant to a large variety of physiological processes. It is appealing to speculate that information about ion concentrations and ion gradients might be mediated to interacting proteins via pore-dependent channel-gating mechanisms.

Outlook for new progress

This Viewpoint has highlighted intrinsic regulatory processes of Na transporters that have received relatively little attention and whose structural basis remains largely or completely unknown. Nevertheless, the inactivation mechanisms discussed are central to an understanding of Na homeostasis and the regulation Na transporter function in mammalian cells. Both Na/Ca exchange and Na/K pumps are regulated by cytoplasmic Na in a steep fashion that is likely linked functionally to Na binding in transport sites when they are open to the cytoplasmic side. The regulation of Na/Ca exchangers by an intrinsic Na-dependent inactivation reaction is in turn regulated by lipid signaling. It still remains to be determined whether inactivation might modify specific ion translocation steps in the exchange cycle (Kang and Hilgemann, 2004). For Na/K pumps, it is striking that Na/K pump inactivation appears to be lost in giant excised patches in an ATP-dependent manner (Friedrich et al., 1996; Hilgemann, 1997). How the inactivation is relieved in response to an elevation of cytoplasmic Ca (Fig. 5) remains completely unknown. Remarkably similar enigmas exist for ENaC Na channels. ENaCs undergo strong Na-dependent inactivation that is progressively lost when oocytes are studied in the cut-open configuration. Enigmas for Na/H exchange (NHE1) regulation are even more challenging. NHE1 function is completely lost in excised patches (Fuster et al., 2004), and it remains unclear whether this loss involves loss of soluble regulators, membrane stretch, or some other regulatory feature. One or more G proteins may well play important roles in Na-sensing (Ash et al., 2012) that regulates both NHEs (Ishibashi et al., 1999; Hilgemann et al., 2006) and ENaC Na channels. However, available data suggests that for ENaCs, G-protein involvement is not obligatory (Hübner et al., 1999). In summary, regulation of Na transport in mammalian cells is a long-established and well-ploughed field, but many profound physiological enigmas remain. The thrust of this Viewpoint has been to highlight enigmas, which appear to reflect signaling that originates via occupation of Na transport sites. The principles discussed will clearly extend to the regulation of other transporters and ion channels.

Online supplemental material

The online supplemental material provides the equations sets used to simulate experimental results, together with the parameters employed in the simulations presented.

Acknowledgments

Merritt C. Maduke served as editor.

I dedicate the article to the memory of David C. Gadsby, my friend, critic, and inspiration to do better.

This work was supported by National Institutes of Health grant RO1HL119843.

The author declares no competing financial interests.

References

- Abriel, H., and J.D. Horisberger. 1999. Feedback inhibition of rat amiloride-sensitive epithelial sodium channels expressed in *Xenopus laevis* oocytes. *J. Physiol.* 516:31–43. <https://doi.org/10.1111/j.1469-7793.1999.031aa.x>
- Aharonovitz, O., N. Demaurex, M. Woodside, and S. Grinstein. 1999. ATP dependence is not an intrinsic property of Na⁺/H⁺ exchanger NHE1: requirement for an ancillary factor. *Am. J. Physiol.* 276:C1303–C1311. <https://doi.org/10.1152/ajpcell.1999.276.6.C1303>
- Aharonovitz, O., H.C. Zaun, T. Balla, J.D. York, J. Orlowski, and S. Grinstein. 2000. Intracellular pH regulation by Na⁺/H⁺ exchange requires phosphatidylinositol 4,5-bisphosphate. *J. Cell Biol.* 150:213–224. <https://doi.org/10.1083/jcb.150.1.213>
- Aronson, P.S., J. Nee, and M.A. Suhm. 1982. Modifier role of internal H⁺ in activating the Na⁺-H⁺ exchanger in renal microvillus membrane vesicles. *Nature.* 299:161–163. <https://doi.org/10.1038/299161a0>
- Ash, M.-R., M.J. Maher, J.M. Guss, and M. Jormakka. 2012. The cation-dependent G-proteins: In a class of their own. *FEBS Letters.* 586: 2218–2224. <https://doi.org/10.1016/j.febslet.2012.06.030>
- Backx, P.H., W.D. Gao, M.D. Azan-Backx, and E. Marban. 1995. The relationship between contractile force and intracellular [Ca²⁺] in intact rat cardiac trabeculae. *J. Gen. Physiol.* 105:1–19. <https://doi.org/10.1085/jgp.105.1.1>
- Bastié, M.J., and J.A. Williams. 1990. Gastrointestinal peptides activate Na⁺-H⁺ exchanger in AR42J cells by increasing its affinity for intracellular H⁺. *Am. J. Physiol.* 258:G958–G966. <https://doi.org/10.1152/ajpgi.1990.258.6.G958>
- Bianchini, L., G. L'Allemain, and J. Pouyssegur. 1997. The p42/p44 mitogen-activated protein kinase cascade is determinant in mediating activation of the Na⁺/H⁺ exchanger (NHE1 isoform) in response to growth factors. *J. Biol. Chem.* 272:271–279. <https://doi.org/10.1074/jbc.272.1.271>
- Blostein, R., and M. Mallet. 1995. ADP controls the electrogenicity of Na/Na exchange catalyzed by dog kidney Na,K-ATPase proteoliposomes. *Biochim. Biophys. Acta.* 1234:1–4. [https://doi.org/10.1016/0005-2736\(94\)00261-M](https://doi.org/10.1016/0005-2736(94)00261-M)
- Carmeliet, E. 1992. A fuzzy subsarcolemmal space for intracellular Na⁺ in cardiac cells? *Cardiovasc. Res.* 26:433–442. <https://doi.org/10.1093/cvr/26.5.433>
- Chen, T.Y. 2003. Coupling gating with ion permeation in ClC channels. *Sci. STKE.* 2003:pe23. <https://doi.org/10.1126/stke.2003.188.pe23>
- Chen, T.Y., and C. Miller. 1996. Nonequilibrium gating and voltage dependence of the ClC-0 Cl⁻ channel. *J. Gen. Physiol.* 108:237–250. <https://doi.org/10.1085/jgp.108.4.237>
- Chraïbi, A., and J.D. Horisberger. 2002. Na self inhibition of human epithelial Na channel: temperature dependence and effect of extracellular proteases. *J. Gen. Physiol.* 120:133–145. <https://doi.org/10.1085/jgp.20028612>
- Chu, L., J.L. Greenstein, and R.L. Winslow. 2019. Na⁺ microdomains and sparks: Role in cardiac excitation-contraction coupling and arrhythmias in ankyrin-B deficiency. *J. Mol. Cell. Cardiol.* 128:145–157. <https://doi.org/10.1016/j.yjmcc.2019.02.001>
- Clausen, M.V., F. Hilbers, and H. Poulsen. 2017. The Structure and Function of the Na,K-ATPase Isoforms in Health and Disease. *Front. Physiol.* 8:371. <https://doi.org/10.3389/fphys.2017.00371>
- Collier, D.M., V.R. Tomkovicz, Z.J. Peterson, C.J. Benson, and P.M. Snyder. 2014. Intersubunit conformational changes mediate epithelial sodium channel gating. *J. Gen. Physiol.* 144:337–348. <https://doi.org/10.1085/jgp.201411208>
- Dinudom, A., K.F. Harvey, P. Komwatana, J.A. Young, S. Kumar, and D.I. Cook. 1998. Nedd4 mediates control of an epithelial Na⁺ channel in salivary duct cells by cytosolic Na⁺. *Proc. Natl. Acad. Sci. USA.* 95: 7169–7173. <https://doi.org/10.1073/pnas.95.12.7169>
- Dixit, M., S. Kim, G.F. Matthews, K. Erreger, A. Galli, C.E. Cobb, E.J. Hustedt, and A.H. Beth. 2013. Structural arrangement of the intracellular Ca²⁺ binding domains of the cardiac Na⁺/Ca²⁺ exchanger (NCX1.1): effects of Ca²⁺ binding. *J. Biol. Chem.* 288:4194–4207. <https://doi.org/10.1074/jbc.M112.423293>
- Dobrunz, L.E., P.H. Backx, and D.T. Yue. 1995. Steady-state [Ca²⁺]_i-force relationship in intact twitching cardiac muscle: direct evidence for modulation by isoproterenol and EMD 53998. *Biophys. J.* 69:189–201. [https://doi.org/10.1016/S0006-3495\(95\)79889-7](https://doi.org/10.1016/S0006-3495(95)79889-7)
- Forsberg, H., and P.O. Ljungdahl. 2001. Sensors of extracellular nutrients in *Saccharomyces cerevisiae*. *Curr. Genet.* 40:91–109. <https://doi.org/10.1007/s002940100244>
- Friedrich, T., E. Bamberg, and G. Nagel. 1996. Na⁺,K⁺-ATPase pump currents in giant excised patches activated by an ATP concentration jump. *Biophys. J.* 71:2486–2500. [https://doi.org/10.1016/S0006-3495\(96\)79442-0](https://doi.org/10.1016/S0006-3495(96)79442-0)
- Fuchs, W., E.H. Larsen, and B. Lindemann. 1977. Current-voltage curve of sodium channels and concentration dependence of sodium permeability in frog skin. *J. Physiol.* 267:137–166. <https://doi.org/10.1113/jphysiol.1977.sp011805>
- Fuster, D., O.W. Moe, and D.W. Hilgemann. 2004. Lipid- and mechano-sensitivities of sodium/hydrogen exchangers analyzed by electrical methods. *Proc. Natl. Acad. Sci. USA.* 101:10482–10487. <https://doi.org/10.1073/pnas.0403930101>
- Fuster, D., O.W. Moe, and D.W. Hilgemann. 2008. Steady-state function of the ubiquitous mammalian Na/H exchanger (NHE1) in relation to dimer coupling models with 2Na/2H stoichiometry. *J. Gen. Physiol.* 132: 465–480. <https://doi.org/10.1085/jgp.200810016>
- Glynn, I.M., and S.J. Karlish. 1976. ATP hydrolysis associated with an uncoupled sodium flux through the sodium pump: evidence for allosteric effects of intracellular ATP and extracellular sodium. *J. Physiol.* 256: 465–496. <https://doi.org/10.1113/jphysiol.1976.sp011333>
- Green, J., D.T. Yamaguchi, C.R. Kleeman, and S. Muallem. 1988. Cytosolic pH regulation in osteoblasts. Interaction of Na⁺ and H⁺ with the extracellular and intracellular faces of the Na⁺/H⁺ exchanger. *J. Gen. Physiol.* 92:239–261. <https://doi.org/10.1085/jgp.92.2.239>
- Grinstein, S., S. Cohen, J.D. Goetz, A. Rothstein, and E.W. Gelfand. 1985. Characterization of the activation of Na⁺/H⁺ exchange in lymphocytes by phorbol esters: change in cytoplasmic pH dependence of the antiport. *Proc. Natl. Acad. Sci. USA.* 82:1429–1433. <https://doi.org/10.1073/pnas.82.5.1429>
- Hilge, M., J. Aelen, A. Foorce, A. Perrakis, and G.W. Vuister. 2009. Ca²⁺ regulation in the Na⁺/Ca²⁺ exchanger features a dual electrostatic switch mechanism. *Proc. Natl. Acad. Sci. USA.* 106:14333–14338. <https://doi.org/10.1073/pnas.0902171106>
- Hilgemann, D.W. 1990. Regulation and deregulation of cardiac Na⁺-Ca²⁺ exchange in giant excised sarcolemmal membrane patches. *Nature.* 344: 242–245. <https://doi.org/10.1038/344242a0>
- Hilgemann, D.W. 1997. Cytoplasmic ATP-dependent regulation of ion transporters and channels: mechanisms and messengers. *Annu. Rev. Physiol.* 59:193–220. <https://doi.org/10.1146/annurev.physiol.59.1.193>
- Hilgemann, D.W. 2019. Control of Cardiac Contraction by Sodium: Promises, Reckonings, and New Beginnings. *Cell Calcium.* <https://doi.org/10.1016/j.ceca.2019.102129>
- Hilgemann, D.W., and R. Ball. 1996. Regulation of cardiac Na⁺,Ca²⁺ exchange and KATP potassium channels by PIP₂. *Science.* 273:956–959. <https://doi.org/10.1126/science.273.5277.956>
- Hilgemann, D.W., and A. Collins. 1992. Mechanism of cardiac Na⁺-Ca²⁺ exchange current stimulation by MgATP: possible involvement of aminophospholipid translocase. *J. Physiol.* 454:59–82. <https://doi.org/10.1113/jphysiol.1992.sp019254>
- Hilgemann, D.W., and C.C. Lu. 1998. Giant membrane patches: improvements and applications. *Methods Enzymol.* 293:267–280. [https://doi.org/10.1016/S0076-6879\(98\)93018-X](https://doi.org/10.1016/S0076-6879(98)93018-X)
- Hilgemann, D.W., A. Collins, and S. Matsuoka. 1992a. Steady-state and dynamic properties of cardiac sodium-calcium exchange. Secondary modulation by cytoplasmic calcium and ATP. *J. Gen. Physiol.* 100: 933–961. <https://doi.org/10.1085/jgp.100.6.933>
- Hilgemann, D.W., S. Matsuoka, G.A. Nagel, and A. Collins. 1992b. Steady-state and dynamic properties of cardiac sodium-calcium exchange. Sodium-dependent inactivation. *J. Gen. Physiol.* 100:905–932. <https://doi.org/10.1085/jgp.100.6.905>
- Hilgemann, D.W., A. Yaradanakul, Y. Wang, and D. Fuster. 2006. Molecular control of cardiac sodium homeostasis in health and disease. *J. Cardiovasc. Electrophysiol.* 17(s1, Suppl 1):S47–S56. <https://doi.org/10.1111/j.1540-8167.2006.00383.x>
- Hooley, R., C.Y. Yu, M. Symons, and D.L. Barber. 1996. G alpha 13 stimulates Na⁺-H⁺ exchange through distinct Cdc42-dependent and RhoA-dependent pathways. *J. Biol. Chem.* 271:6152–6158. <https://doi.org/10.1074/jbc.271.11.6152>
- Hübner, M., R. Schreiber, A. Boucherot, A. Sanchez-Perez, P. Poronnik, D.I. Cook, and K. Kunzelmann. 1999. Feedback inhibition of epithelial Na⁺

- channels in *Xenopus* oocytes does not require G(0) or G(i2) proteins. *FEBS Lett.* 459:443–447. [https://doi.org/10.1016/S0014-5793\(99\)01291-0](https://doi.org/10.1016/S0014-5793(99)01291-0)
- Inesi, G., and F. Tadini-Buoninsegni. 2014. Ca(2+)/H(+) exchange, luminal Ca(2+) release and Ca(2+)/ATP coupling ratios in the sarcoplasmic reticulum ATPase. *J. Cell Commun. Signal.* 8:5–11. <https://doi.org/10.1007/s12079-013-0213-7>
- Ishibashi, H., A. Dinudom, K.F. Harvey, S. Kumar, J.A. Young, and D.I. Cook. 1999. Na(+)-H(+) exchange in salivary secretory cells is controlled by an intracellular Na(+) receptor. *Proc. Natl. Acad. Sci. USA.* 96:9949–9953. <https://doi.org/10.1073/pnas.96.17.9949>
- Ishihara, K. 2018. External K⁺ dependence of strong inward rectifier K⁺ channel conductance is caused not by K⁺ but by competitive pore blockade by external Na. *J. Gen. Physiol.* 150:977–989. <https://doi.org/10.1085/jgp.201711936>
- Jackson, W.F. 2017. Boosting the signal: Endothelial inward rectifier K(+) channels. *Microcirculation.* 24:10.1111/micc.12319.
- Jean, T., C. Frelin, P. Vigne, P. Barbry, and M. Lazdunski. 1985. Biochemical properties of the Na⁺/H⁺ exchange system in rat brain synaptosomes. Interdependence of internal and external pH control of the exchange activity. *J. Biol. Chem.* 260:9678–9684.
- Jentsch, T.J., and M. Pusch. 2018. CLC Chloride Channels and Transporters: Structure, Function, Physiology, and Disease. *Physiol. Rev.* 98:1493–1590. <https://doi.org/10.1152/physrev.00047.2017>
- Kang, T.M., and D.W. Hilgemann. 2004. Multiple transport modes of the cardiac Na⁺/Ca²⁺ exchanger. *Nature.* 427:544–548. <https://doi.org/10.1038/nature02271>
- Kang, T.M., V.S. Markin, and D.W. Hilgemann. 2003. Ion fluxes in giant excised cardiac membrane patches detected and quantified with ion-selective microelectrodes. *J. Gen. Physiol.* 121:325–347. <https://doi.org/10.1085/jgp.200208777>
- Kashlan, O.B., B.M. Blobner, Z. Zuzek, M. Tolino, and T.R. Kleyman. 2015. Na⁺ inhibits the epithelial Na⁺ channel by binding to a site in an extracellular acidic cleft. *J. Biol. Chem.* 290:568–576. <https://doi.org/10.1074/jbc.M114.606152>
- Lederer, W.J., E. Niggli, and R.W. Hadley. 1990. Sodium-calcium exchange in excitable cells: fuzzy space. *Science.* 248:283. <https://doi.org/10.1126/science.2326638>
- Lee, B.L., B.D. Sykes, and L. Fliegel. 2013. Structural and functional insights into the cardiac Na⁺/H⁺ exchanger. *J. Mol. Cell. Cardiol.* 61:60–67. <https://doi.org/10.1016/j.yjmcc.2012.11.019>
- Lin, X., T.A. Voyno-Yasenetskaya, R. Hooley, C.Y. Lin, J. Orlowski, and D.L. Barber. 1996. Galphal2 differentially regulates Na⁺/H⁺ exchanger isoforms. *J. Biol. Chem.* 271:22604–22610. <https://doi.org/10.1074/jbc.271.37.22604>
- Lin, C.Y., M.G. Varma, A. Joubel, S. Madabushi, O. Lichtarge, and D.L. Barber. 2003. Conserved motifs in somatostatin, D2-dopamine, and alpha 2B-adrenergic receptors for inhibiting the Na-H exchanger, NHE1. *J. Biol. Chem.* 278:15128–15135. <https://doi.org/10.1074/jbc.M212315200>
- Ling, G.N.. 1965. Physiology and anatomy of the cell membrane: the physical state of water in the living cell. *Fed. Proc.* 24:S103–S112.
- Lu, F.M., and D.W. Hilgemann. 2017. Na/K pump inactivation, subsarcolemmal Na measurements, and cytoplasmic ion turnover kinetics contradict restricted Na spaces in murine cardiac myocytes. *J. Gen. Physiol.* 149:727–749. <https://doi.org/10.1085/jgp.201711780>
- Lu, F.M., C. Deisl, and D.W. Hilgemann. 2016. Profound regulation of Na/K pump activity by transient elevations of cytoplasmic calcium in murine cardiac myocytes. *eLife.* 5:e19267. <https://doi.org/10.7554/eLife.19267>
- Matsuoka, S., and D.W. Hilgemann. 1994. Inactivation of outward Na(+)-Ca2+ exchange current in guinea-pig ventricular myocytes. *J. Physiol.* 476:443–458. <https://doi.org/10.1113/jphysiol.1994.sp020146>
- Matsuoka, S., D.A. Nicoll, R.F. Reilly, D.W. Hilgemann, and K.D. Philipson. 1993. Initial localization of regulatory regions of the cardiac sarcolemmal Na(+)-Ca2+ exchanger. *Proc. Natl. Acad. Sci. USA.* 90:3870–3874. <https://doi.org/10.1073/pnas.90.9.3870>
- Ottolia, M., and K.D. Philipson. 2013. NCX1: mechanism of transport. *Adv. Exp. Med. Biol.* 961:49–54. https://doi.org/10.1007/978-1-4614-4756-6_5
- Philipson, K.D., D.A. Nicoll, M. Ottolia, B.D. Quednau, H. Reuter, S. John, and Z. Qiu. 2002. The Na⁺/Ca²⁺ exchange molecule: an overview. *Ann. N. Y. Acad. Sci.* 976:1–10. <https://doi.org/10.1111/j.1749-6632.2002.tb04708.x>
- Requena, J. 1978. Calcium efflux from squid axons under constant sodium electrochemical gradient. *J. Gen. Physiol.* 72:443–470. <https://doi.org/10.1085/jgp.72.4.443>
- Schewe, M., E. Nematian-Ardestani, H. Sun, M. Musinszki, S. Cordeiro, G. Bucci, B.L. de Groot, S.J. Tucker, M. Rapedius, and T. Baukrowitz. 2016. A Non-canonical Voltage-Sensing Mechanism Controls Gating in K2P K(+) Channels. *Cell.* 164:937–949. <https://doi.org/10.1016/j.cell.2016.02.002>
- Skou, J.C. 1998. The Identification of the Sodium-Potassium Pump (Nobel Lecture). *Angew. Chem. Int. Ed. Engl.* 37:2320–2328. [https://doi.org/10.1002/\(SICI\)1521-3773\(19980918\)37:17<2320::AID-ANIE2320>3.0.CO;2-2](https://doi.org/10.1002/(SICI)1521-3773(19980918)37:17<2320::AID-ANIE2320>3.0.CO;2-2)
- Tal, I., T. Kozlovsky, D. Brisker, M. Giladi, and D. Khananshvil. 2016. Kinetic and equilibrium properties of regulatory Ca(2+)-binding domains in sodium-calcium exchangers 2 and 3. *Cell Calcium.* 59:181–188. <https://doi.org/10.1016/j.ceca.2016.01.008>
- Vaughan-Jones, R.D., and M.L. Wu. 1990. Extracellular H⁺ inactivation of Na(+)-H⁺ exchange in the sheep cardiac Purkinje fibre. *J. Physiol.* 428:441–466. <https://doi.org/10.1113/jphysiol.1990.sp018221>
- Wakabayashi, S., T. Hisamitsu, T. Pang, and M. Shigekawa. 2003. Kinetic dissection of two distinct proton binding sites in Na⁺/H⁺ exchangers by measurement of reverse mode reaction. *J. Biol. Chem.* 278:43580–43585. <https://doi.org/10.1074/jbc.M306690200>
- Wendt-Gallitelli, M.F., T. Voigt, and G. Isenberg. 1993. Microheterogeneity of subsarcolemmal sodium gradients. Electron probe microanalysis in guinea-pig ventricular myocytes. *J. Physiol.* 472:33–44. <https://doi.org/10.1113/jphysiol.1993.sp019934>

Supplemental material

Hilgemann, <https://doi.org/10.1085/jgp.201912455>

Description of simulations

All simulations were performed in MATLAB. Equation sets employed were as follows.

NCX simulations

Exchangers are assumed to exist in four states (F_1 - F_4). F_1 is the inactive state with a bound regulatory Ca and closed PIP₂ gate. F_2 is the active state. F_3 is the inactive state with a bound Ca and open PIP₂ gate. F_4 is the inactive state without regulatory Ca and closed PIP₂ gate. Full occupation of three Na transport sites (F_{3n}) is assumed to be proportional to a Hill equation with a slope of 2.5 and a K_{50} for Na (N_i) of 17 mM. Both outward exchange current (Incx) transport and inactivation via the PIP₂ gate are proportional to F_{3n} .

$$F_{3n} = N_i^{2.5} / (N_i^{2.5} + 17^{2.5}), \quad (1)$$

$$dF_1/dt = F_4 \times C_i \times K_{con1} - F_1 \times K_{coff1} + F_2 \times F_{3n} \times K_{inact1} - F_1 \times K_{12}, \quad (2)$$

$$dF_2/dt = F_3 \times C_i \times K_{con2} - F_2 \times K_{con2} + F_1 \times K_{12} - F_2 \times F_{3n} \times K_{inact1}, \quad (3)$$

$$dF_3/dt = F_2 \times K_{coff2} + F_4 \times K_{43} - F_3 \times C_i \times K_{con2} - F_3 \times F_{3n} \times K_{inact2}, \quad (4)$$

$$F_4 = 1 - F_1 - F_2 - F_3, \quad (5)$$

$$I_{ncx} = F_2 \times F_{3n}. \quad (6)$$

Parameter settings for Fig. 2

$K_{con1} = 0.1 \mu\text{M}^{-1}\text{s}^{-1}$; $K_{coff1} = 0.05 \mu\text{M}^{-1}\text{s}^{-1}$; $K_{con2} = 20 \text{ s}^{-1}$; $K_{coff2} = 0.3 \text{ s}^{-1}$; $K_{inact1} = 0.2 \text{ s}^{-1}$; $K_{inact2} = K_{inact1} \times 25 \text{ s}^{-1}$; $K_{12} = 0.2 \text{ s}^{-1}$; $K_{43} = 0.1 \text{ s}^{-1}$. Note that the two Na-dependent inactivation reactions are assumed to both be regulated by anionic phospholipids in the simulation presented.

Na/K pump simulations

The minimal Na/K pump model employed assumes that two Na and two K bind competitively in both E_1 and E_2 configurations and that a third Na ion binds independently at a separate site. 90% of voltage dependence is partitioned to extracellular Na binding to the Na-selective site, and 10% is partitioned to reactions that translocate three Na. Na translocation rates are simulated to be twice faster than K translocation. The simulated Na/K pump activity reproduces the concentration and voltage dependencies of Na/K pumps in reasonable approximation, and the model is consistent with a free energy of ATP hydrolysis of 52 kJ/mol under the conditions simulated. Inactivation occurs from all E_1 Na sites that are not fully occupied, and recovery occurs from fully Na occupied E_1 sites.

F_{no} , F_{ni} , F_{n2o} , F_{n2i} , F_{k2o} , and F_{k2i} give the fractional occupation of ion-binding sites; F_{ATP} , F_{pi} and F_{ADP} give the fractional occupation of nucleotide and phosphate sites; and D_i , D_o , K_1 , K_2 , K_3 , and K_4 are temporary variables. Na and K binding are mutually exclusive, as are ATP and P_i binding. E_m is in millivolts. N_o , K_o , N_i , and K_i are the extracellular and intracellular Na and K concentrations, and the 10 ion dissociation constants are designated with parameter settings.

$$F_{no} = N_o / (N_o + K_{no3} \times e^{E_m/26 \times 0.9}), \quad (7)$$

$$D_o = 1 + N_o / K_{no1} \times (1 + N_o / K_{no2}) + K_o / K_{ko1} \times (1 + K_o / K_{ko2}), \quad (8)$$

$$F_{k2o} = K_o \times K_o / K_{ko1} / K_{ko2} / D_o, \quad (9)$$

$$F_{n2o} = N_o \times N_o / K_{no1} / K_{no2} / D_o, \quad (10)$$

$$F_{ni} = N_i / (N_i + K_{ni3}), \quad (11)$$

$$D_i = 1 + N_i / K_{ni1} \times (1 + N_i / K_{ni2}) + K_i / K_{ki1} \times (1 + K_i / K_{ki2}), \quad (12)$$

$$F_{k2i} = K_i \times K_i / K_{ki1} / K_{ki2} / D_i, \quad (13)$$

$$F_{n2i} = N_i \times N_i / K_{ni1} / K_{ni2} / D_i, \quad (14)$$

$$F_{ADP} = ADP / (ADP + K_{ADP}), \quad (15)$$

$$F_{ATP} = ATP / K_{ATP} / (1 + ATP / K_{ATP} + P_i / K_{pi}), \quad (16)$$

$$F_{pi} = P_i / K_{pi} / (1 + ATP / K_{ATP} + P_i / K_{pi}), \quad (17)$$

$$K_1 = 2 \times F_{ni} \times F_{n2i} \times F_{ATP} \times (1 - F_{ADP}) \times e^{E_m/55 \times 0.1}, \quad (18)$$

$$K_2 = 2 \times F_{no} \times F_{n2o} \times (F_{ADP} + 0.32) \times e^{-E_m/55 \times 0.1}, \quad (19)$$

$$K_3 = F_{k2o} \times (1 - F_{no}), \quad (20)$$

$$K_4 = F_{k2i} \times F_{pi} \times (1 - F_{ni}), \quad (21)$$

$$E_2 = (K_1 + K_4) / (K_1 + K_2 + K_3 + K_4), \quad (22)$$

$$E_1 = 1 - E_2. \quad (23)$$

From the E_1 and E_2 fractions, a fractional pump activity, Pump, was calculated:

$$\text{Pump} = E_1 \times K_1 - E_2 \times K_2. \quad (24)$$

Inactivation was simulated as the fraction of pumps in the active state (F_{act}):

$$dF_{act}/dt = (1 - F_{act}) \times F_{n2i} \times F_{ni} \times K_{rec} - E_1 \times F_{act} \times ((1 - F_{n2i}) + (1 - F_{ni})) \times K_{inact}. \quad (25)$$

The pump current is then

$$I_{pump} = \text{Pump} \times F_{act} \times K_{pump}. \quad (26)$$

For results presented in Fig. 6, the cytoplasmic Na concentration (N_i) was simulated assuming a constant background Na current (I_{na}), a 10-pI cytoplasmic mixing volume, and an exchange time constant between the pipette and cytoplasm, τ_{pip} , of 12 s.

With the pipette Na concentration being Na_{pip} , cytoplasmic Na is simulated as:

$$dN_i/dt = (I_{na} - I_{pump} \times 3) / 1,000 + (Na_{pip} - N_i) / \tau_{pip}. \quad (27)$$

Parameter settings for Fig. 6

$Na_{pip} = 20$ mM; $N_o = 120$ mM; $K_o = 7.0$ mM; $K_i = 120$ mM; $ADP = 0.05$ mM; $P_i = 0.3$ mM; $ATP = 6$ mM; $Na_{pip} = 20$ mM; $E_m = 0$ mV; $\tau_{pip} = 12$ s; $K_{rec} = 0.8$ s⁻¹; $K_{pump} = 2.5$ nA; $K_{no3} = 900$ mM; $K_{no1} = 10$ mM; $K_{no2} = 10$ mM; $K_{ko1} = 0.3$ mM; $K_{ko2} = 0.2$ mM; $K_{ni3} = 4$ mM; $K_{ni1} = 6$ mM; $K_{ni2} = 6$ mM; $K_{ki1} = 20$ mM; $K_{ki2} = 30$ mM; $K_{ATP} = 0.08$ mM; $K_{ADP} = 2$ mM; $K_{pi} = 5$ mM; $K_{inact} = 1.9$ or 0.24 s⁻¹.

Parameter settings for Fig. 7

Na exchange to the pipette tip was omitted, and the following parameter changes were employed: $E_m = -80$ mV; $K_{inact} = 2$ s⁻¹; $K_{rec} = 40$ s⁻¹; $K_{pump} = 1$ nA in absence of inactivation; $K_{pump} = 4$ nA with inactivation.

Na/H exchange simulations

For the simulations in Fig. 9, Na/H exchange was assumed to take place by a simple consecutive mechanism with the same extracellular and cytoplasmic Na and H dissociation constants (K_h and K_n), with the same Na and H translocation rates in both directions, and with Na and H binding occurring competitively. The fractions of bindings sites occupied by H and Na (F_{no} , F_{ni} , F_{ho} , and F_{hi}) were first calculated:

$$D_o = 1 + N_o/K_n + H_o/K_h, \quad (28)$$

$$F_{no} = N_o/K_n/D_o, \quad (29)$$

$$F_{ho} = H_o/K_h/D_o, \quad (30)$$

$$D_i = 1 + N_i/K_n + H_i/K_h, \quad (31)$$

$$F_{ni} = N_i/K_n/D_i, \quad (32)$$

$$F_{hi} = H_i/K_h/D_i. \quad (33)$$

Then, the fractions of transporters open to the outside (E_2) and inside (E_1) were calculated, as well as transport rate that is independent of inactivation, as a fractional maximal translocation rate (F_{max}):

$$E_2 = (F_{ni} + F_{hi}) / (F_{ni} + F_{hi} + F_{no} + F_{ho}), \quad (34)$$

$$E_1 = 1 - E_2, \quad (35)$$

$$F_{max} = (E_2 \times F_{no} - E_1 \times F_{ni}). \quad (36)$$

The simulation assumes that Na must bind at the inactivated transport sites before cytoplasmic protons can bind to regulatory sites on the cytoplasmic side. It also includes the notion that both extracellular and cytoplasmic Na can be effective, assuming that inactive exchangers can be open to either the outside or inside. With a Na dissociation constant of 10 mM and a proton dissociation constant of 0.2 μ M, the fraction of exchangers with 3 protons bound to regulatory sites (F_{3H}) is

$$F_{3H} = (N_o + N_i) / 10 \times H_i^3 / 0.2^3 / (1 + (N_o + N_i) / 10 \times (1 + H_i^3 / 0.2^3)). \quad (37)$$

Assuming that extracellular H binding to transport sites promotes inactivation (i.e., the opening of regulatory sites to the cytoplasmic side) at a rate that is twice faster than the maximal recovery from inactivation, the fraction of active exchangers (F_{act}) becomes

$$F_{\text{act}} = F_{3H}/(F_{3H} + F_{\text{ho}} \times 2). \quad (38)$$

And the fractional transport rate (R_{nhe}) is

$$R_{\text{nhe}} = F_{\text{act}} \times F_{\text{max}}. \quad (39)$$

Parameter settings for Fig. 9

$N_i = 4 \text{ mM}$; $H_o = 0.1 \times 10^{-3} \text{ mM}$; $H_i = 0.12 \times 10^{-3} \text{ mM}$; $K_n = 10 \text{ mM}$; $K_h = 0.1 \times 10^{-3} \text{ mM}$.